

# *Electronic Supplementary Information for*

## **RE-doped (RE = La, Ce and Er) Ni<sub>2</sub>P Porous Nanostructures as Promising Electrocatalysts for Hydrogen Evolution Reaction**

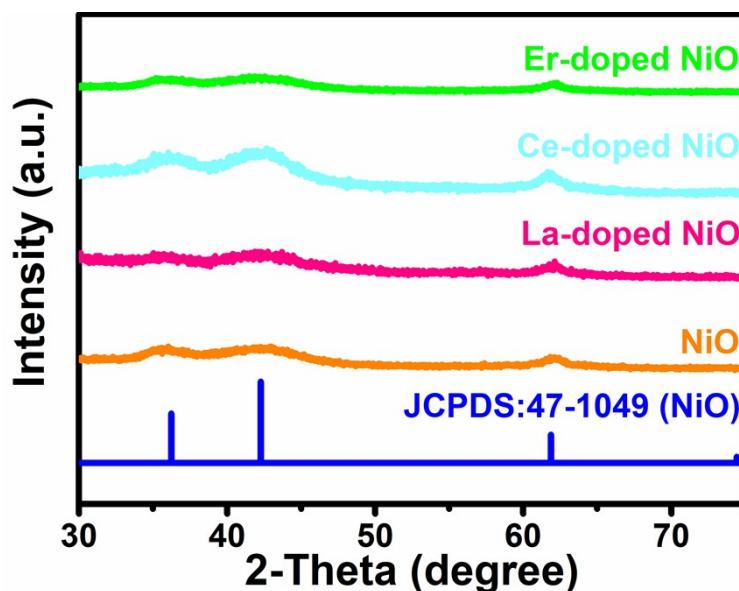


Fig. S1 XRD patterns of NiO and La, Ce and Er-doped NiO nanosheets.

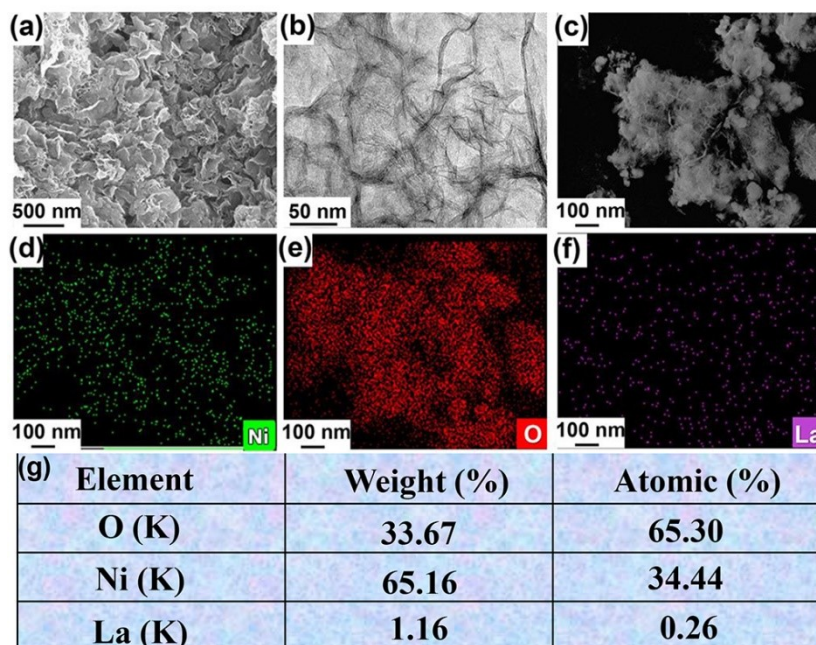


Fig. S2 (a) SEM and (b) TEM images of La-doped NiO nanosheets; (c-f) EDS elemental mappings of Ni, O and La in the La-doped NiO nanosheets; (g) Summary of the element content of La-doped NiO nanosheets after SEM-EDS analysis.

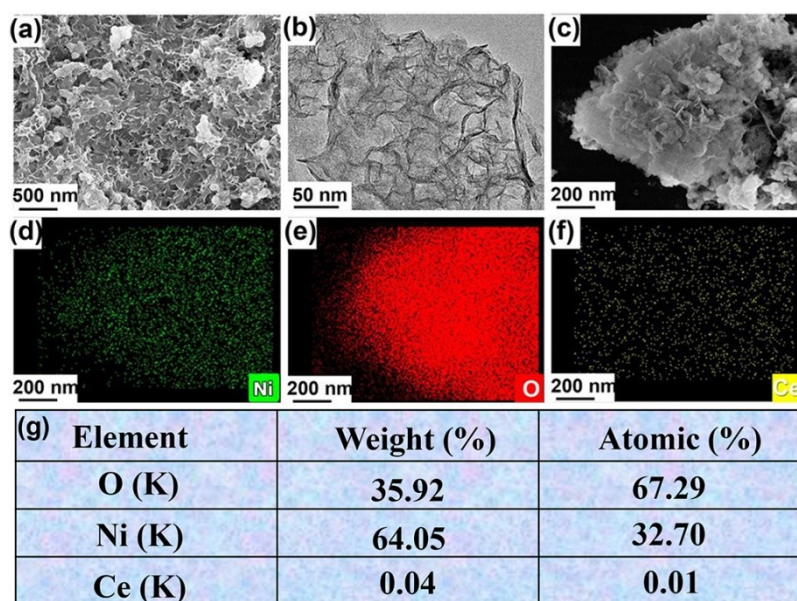


Fig. S3 (a) SEM and (b) TEM images of Ce-doped NiO nanosheets; (c-f) EDS elemental mappings of Ni, O and Ce in the Ce-doped NiO nanosheets. (g) Summary of the element content of Ce-doped NiO nanosheets after SEM-EDS analysis.

Element	Weight (%)	Atomic (%)
O (K)	42.77	75.43
Ni (K)	51.88	22.97
Er (K)	5.35	1.60

Fig. S4 Summary of the element content of Er-doped NiO nanosheets after TEM-EDS analysis.

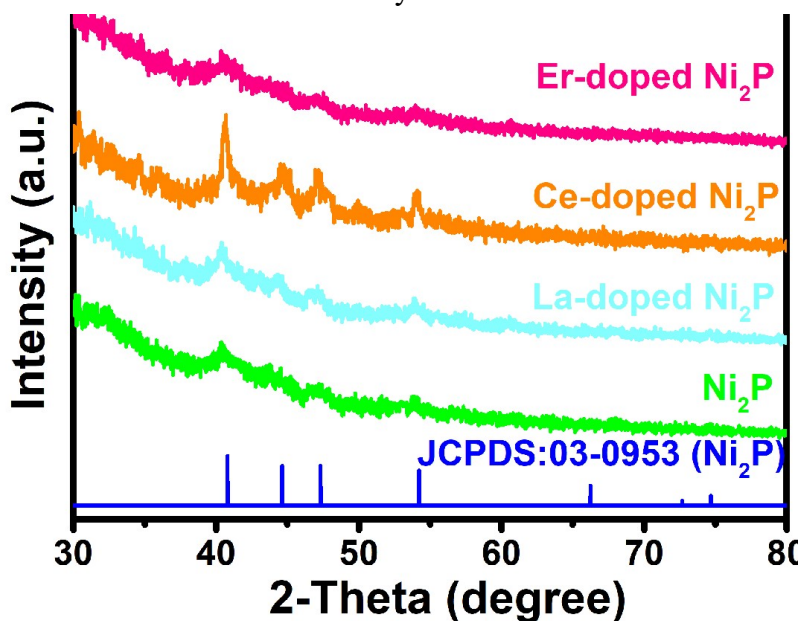


Fig. S5 XRD patterns of Ni<sub>2</sub>P and La, Ce and Er-doped Ni<sub>2</sub>P porous nanostructures.

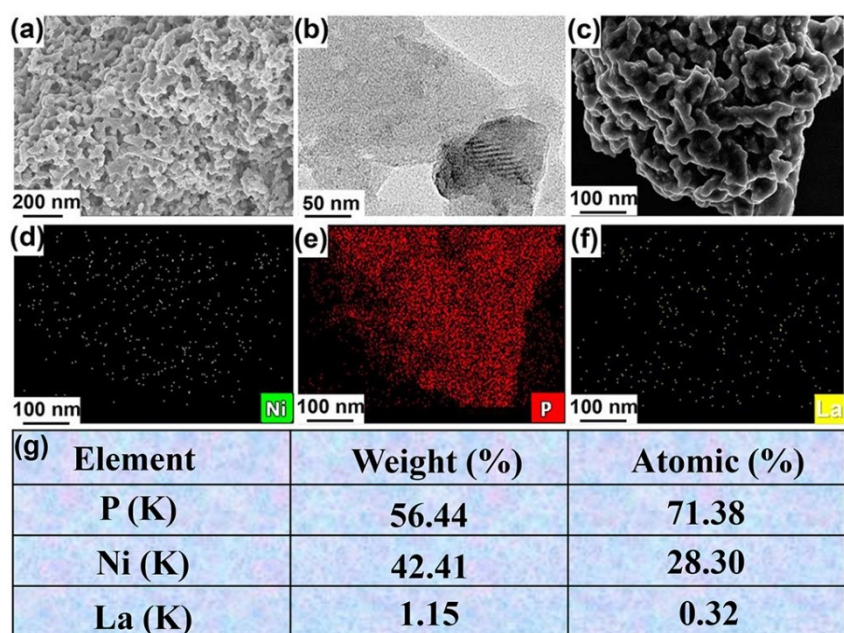


Fig. S6 (a) SEM and (b) TEM images of La-doped  $\text{Ni}_2\text{P}$  porous nanostructures; (c-f) EDS elemental mappings of Ni, P and La in the La-doped  $\text{Ni}_2\text{P}$  porous nanostructures. (g) Summary of the element content of La-doped  $\text{Ni}_2\text{P}$  porous nanostructures after SEM-EDS analysis.

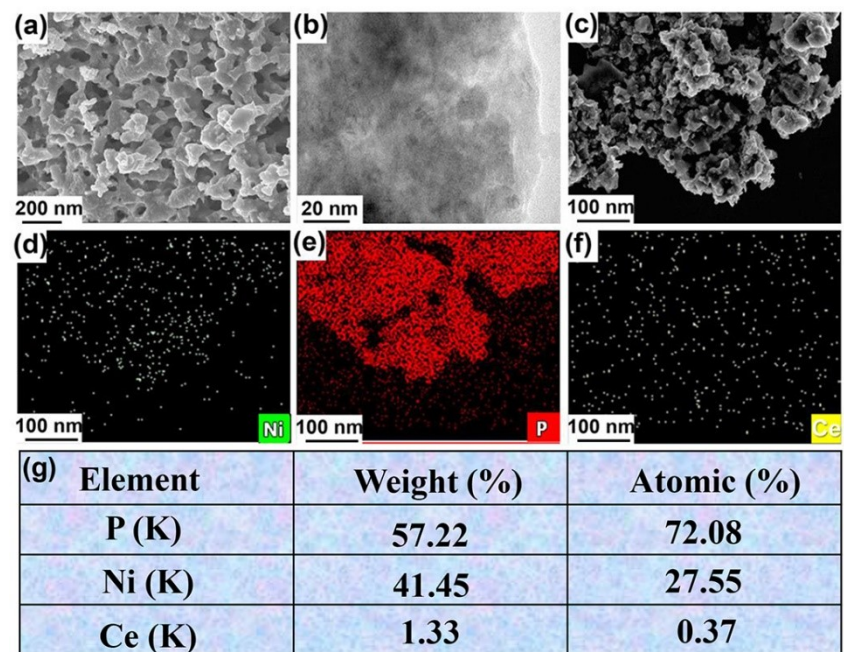


Fig. S7 (a) SEM and (b) TEM images of Ce-doped  $\text{Ni}_2\text{P}$  porous nanostructures; (c-f) EDS elemental mappings of Ni, P and Ce in the Ce-doped  $\text{Ni}_2\text{P}$  porous nanostructures. (g) Summary of the element content of Ce-doped  $\text{Ni}_2\text{P}$  porous nanostructures after SEM-EDS analysis.

Element	Weight (%)	Atomic (%)
P (K)	35.02	53.16
Ni (K)	62.96	44.03
Er (K)	2.02	2.82

Fig. S8 Summary of the element content of Er-doped  $\text{Ni}_2\text{P}$  porous nanostructures after TEM-EDS analysis.

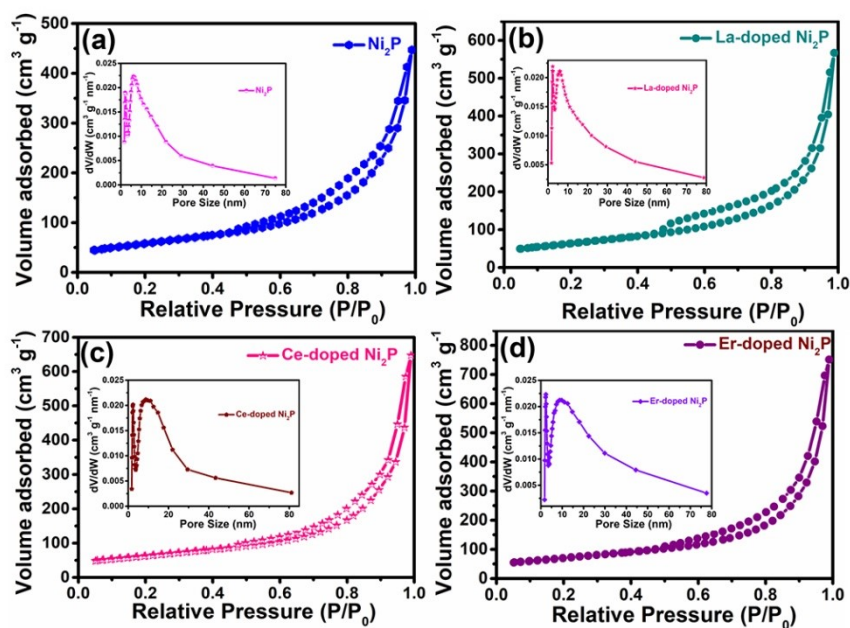


Fig. S9  $\text{N}_2$  adsorption/desorption isotherms of (a) pristine  $\text{Ni}_2\text{P}$ , (b) La-doped  $\text{Ni}_2\text{P}$ , (c) Ce-doped  $\text{Ni}_2\text{P}$  and (d) Er-doped  $\text{Ni}_2\text{P}$  porous nanostructures. Inset: pore size distribution of the corresponding porous nanostructures.

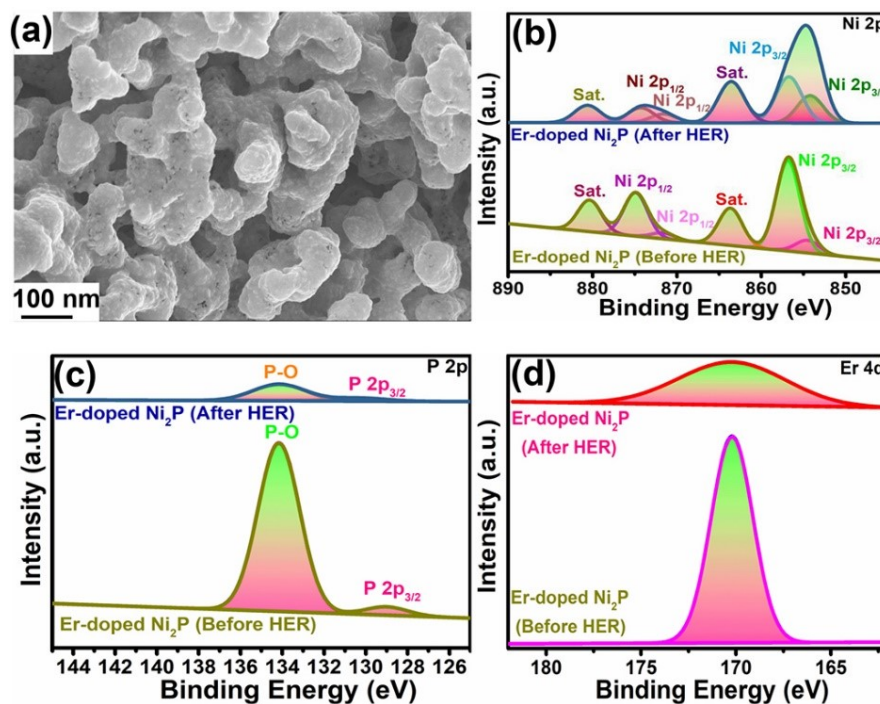


Fig. S10 (a) SEM image of Er-doped  $\text{Ni}_2\text{P}$  porous nanostructures after 30 h HER stability test. XPS signals of (b) Ni 2p, (c) P 2p and (d) Er 4d for the Er-doped  $\text{Ni}_2\text{P}$  porous nanostructures after 30 h HER stability test.

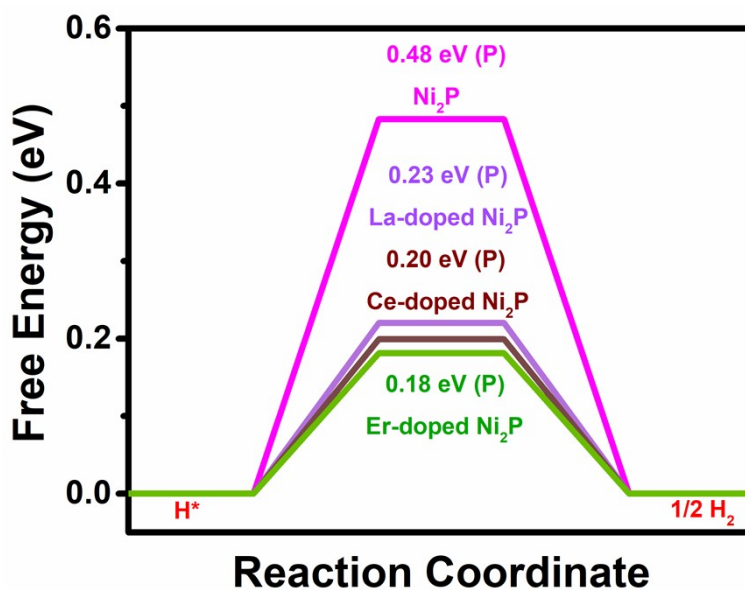


Fig. S11 Free-energy comparison diagram of optimal P active site for HER on (a) pristine  $\text{Ni}_2\text{P}$  (111); (b) La-doped  $\text{Ni}_2\text{P}$  (111); (c) Ce-doped  $\text{Ni}_2\text{P}$  (111); (d) Er-doped  $\text{Ni}_2\text{P}$  (111).